HHS Public Access

Author manuscript

Int J Radiat Oncol Biol Phys. Author manuscript; available in PMC 2020 November 01.

Published in final edited form as:

Int J Radiat Oncol Biol Phys. 2019 November 01; 105(3): 537–547. doi:10.1016/j.ijrobp.2019.06.2533.

Fasting reduces intestinal radiotoxicity enabling dose-escalated radiotherapy for pancreatic cancer

Marimar de la Cruz Bonilla, BS[1,‡], **Kristina M. Stemler, PhD**[1], **Sabrina Jeter-Jones, BS**[1], **Tara N. Fujimoto, BS**[1,3], **Jessica Molkentine, BS**[1,3], **Gabriela M. Asencio Torres**[1], **Xiaomei Zhang, PhD**[1], **Russell R. Broaddus, MD/PhD**[2], **Cullen M. Taniguchi, MD/PhD**[1,3,†,*], **Helen Piwnica-Worms, PhD**[1,†,*]

[1]Department of Experimental Radiation Oncology, The University of Texas MD Anderson Cancer Center, Houston, TX, 77030 USA

[2]Department of Pathology, The University of Texas MD Anderson Cancer Center, Houston, TX, 77030 USA

[3]Department of Radiation Oncology, The University of Texas MD Anderson Cancer Center, Houston, TX, 77030 USA

Abstract

Purpose—Chemotherapy combined with radiotherapy is the most commonly used approach for treating locally advanced pancreatic cancer. The use of curative doses of radiation in this disease setting is constrained due to the close proximity of the head of the pancreas to the duodenum. The purpose of this study was to determine if fasting protects the duodenum from high-dose radiation, thereby enabling dose escalation for efficient killing of pancreatic tumor cells.

Methods and Materials—C57BL/6J mice were either fed or fasted for 24 h and then exposed to total abdominal radiation at 11.5 Gy. Food intake, body weight, overall health and survival were monitored. Small intestines were harvested at various timepoints after radiation and villi length, crypt depth, and number of crypts per mm of intestine were determined. Immunohistochemistry was performed to assess apoptosis and double strand DNA breaks and microcolony assays were peformed to determine intestinal stem cell regeneration capacity. A syngeneic KPC model of pancreatic cancer was employed to determine the effects of fasting on the radiation responses of both pancreatic cancer and host intestinal tissues.

Results—We demonstrated that a 24 h fast in mice improved intestinal stem cell regeneration by microcolony assay and improved host survival from lethal doses of total abdominal radiation when compared to fed controls. Fasting also improved survival of mice with orthotopic pancreatic tumors subjected to lethal abdominal radiation when compared to controls with free access to

*Corresponding authors (ctaniguchi@mdanderson.org, 713-745-5269; hpiwnica-worms@mdanderson.org, 713-794-5717).
†Equal contribution
‡Statistical analysis author (mde4@mdanderson.org, 787-415-2057)

food. Furthermore, fasting did not impact tumor cell killing by radiation therapy and enhanced γ-H2AX staining after radiotherapy, suggesting an additional mild radiosensitizating effect.

Conclusions—These results establish proof-of-concept for fasting as a dose-escalation strategy, enabling ablative radiation in the treatment of unresectable pancreatic cancer.

Introduction

Pancreatic ductal adenocarcinoma (PDAC) is expected to become the most common cause of cancer-related deaths by 2030[1]. There has been little improvement in PDAC prognosis over the last several decades, and the 5-year survival rate of pancreatic cancer remains below 10%[2]. Currently, the most effective treatment for PDAC is surgery. However, because of the late onset of symptoms, only 15–20% of patients present with resectable disease, and the remaining 80%–85% are incurable without appropriate local therapy. Chemotherapy combined with radiotherapy (RT) is the most commonly used approach for treating unresectable pancreatic cancer.

Unfortunately, radiation therapy cannot yet achieve curative doses for pancreatic cancer due to the sensitivity of the nearby gastrointestinal (GI) tract to radiation damage. Results from phase I/II trials have demonstrated that dose escalation is possible with sophisticated radiation techniques like intensity-modulated radiation therapy (IMRT)[3]. Though these conformal techniques are highly precise, they often cannot avoid the duodenum which abuts the pancreas. Moreover, considerable expertise is required for dose-escalated radiation within the abdomen or pelvis, which limits these treatments to a handful of academic centers. Thus, a complementary and potentially more tractable method to improve the therapeutic ratio for chemoradiation for tumors within the abdomen or pelvis may be to reduce toxicity to the GI tract with a radioprotectant.

Interestingly, fasting has been shown to provide host-protective effects from the toxicity associated with high-dose chemotherapy in mice[4,5] and in a patient case series[6]. Importantly, fasting protects small intestinal (SI) stem cells thereby preserving SI homeostasis and promoting organismal survival in the presence of lethal doses of etoposide[5].

In the context of radiation, one study explored the use of prolonged fasting in combination with RT on a subcutaneous mouse model of glioma and reported sensitization of the tumor to radiation[7]. Although the effects of caloric restriction and ketogenic diets on radiation response have been described[8], ours is the first study to examine the effects of short-term fasting on the radiation response of normal tissues. Here, we demonstrate that fasting protects mice from what would otherwise be a lethal dose of RT and we translate our findings to an aggressive mouse model of pancreatic cancer.

Methods and Materials

Study Approval.

This study was carried out in accordance with the recommendations in the Guide for the Care and Use of Laboratory Animals from the NIH and all protocols were approved by our Institutional Animal Care and Use Committee (IACUC). Animals were euthanized as

dictated by the Association for Assessment and Accreditation of Laboratory Animal Care International and IACUC euthanasia endpoints.

Mice.

Both male and female mice were used in this study. C57Bl/6J mice (stock no. 000664) were purchased from The Jackson Laboratory. Nine-week-old male mice used for survival and intestinal histology experiments weighed from 23.4g to 26.6g, whereas female mice ranged from 18.1g to 20.5g.

KPC Cell Growth.

The KPC cell line was derived from a spontaneous tumor from a female *KrasG12D*$^{LSL/+}$; *Trp53 R172H; Pdx1-Cre* (KPC) mouse[9]. KPC cells were maintained in RPMI 1640 (Sigma Aldrich) supplemented with 1% GlutaMAX™, 1% sodium pyruvate, and recombinant insulin (all from Life Technologies). Media was supplemented with 10% regular fetal bovine serum (Heat-inactivated, Atlanta Biologicals).

Orthotopic Injections.

KPC cells were resuspended in RPMI 1640 (Sigma Aldrich) and mixed with chilled Matrigel in a 1:1 ratio. Mice were anesthetized with 2% isoflurane and supported with artificial eye drops and a prophylactic dose of 0.1 mg/kg extended release buprenorphine given subcutaneously for post-operative analgesia. Mice were placed in the right lateral decubitus position, fur was shaved and wiped with a 10% povidone iodine solution and 70% ethanol. Through a 1.5 cm incision with sterile surgical instruments, the spleen was visualized and removed from the abdominal cavity exposing the underlying tail of the pancreas. KPC cells (2×10^4 cells) in 20 μL of Matrigel were injected into the pancreatic parenchyma and observed until the Matrigel solidified. The organs were returned and the abdomen was closed with absorbable 6–0 sutures and surgical staples. Mice were observed as they recovered from their operation. Tumors were allowed to grow for two weeks and then monitored with ultrasound imaging.

Animal Ultrasound.

Mice were subjected to 2% isoflurane for anesthesia, and treated with epilation cream. Animals were then placed onto a Vevo 2100 system (FujiFilm VisualSonics). A 30 MHz transducer was used to acquire B-MODE long and short axis acquisitions[9]. Tumor measurements were made every 4–5 days until animal death or euthanasia.

Small Animal Irradiation.

Small animal irradiation was performed as previously described[10]. Experimental mice were singly housed on aspen bedding. Mice were allowed to feed *ad libitum* or were fasted for 24 h, followed by total abdominal radiation (TA-XRT). Mice were treated on an X-RAD 225Cx machine with an isoflurane anesthesia manifold and on-board image guidance. Beam arrangement was anterior-posterior/posterior-anterior using a 25-mm cone positioned under the xyphoid process through image guidance by cone beam computed tomography. The final dose of TA-XRT was 11.5 Gy for C57Bl/6J non-tumor bearing mice and 12 Gy TA-XRT for

tumor bearing mice. After treatment moistened food pellets were placed at the bottom of all cages.

Immunohistochemistry and Immunofluorescence.

Mouse SI were harvested as described previously[5], and jejunum sections were used for all analyses. Microlony assays were performed using the classical Withers and Elkind technique[11]. Briefly, jejunums were resected, fixed in 10% neutral buffered formalin, paraffin embedded, and cut transversely for subsequent H & E staining and analysis.

Immunofluorescence (IF) staining of tumor tissues for cleaved-caspase 3 (CC3) and γ-H2AX and of SI for Ki67, utilized triology (Cell Marque) for deparafinization, rehydration, and antigen retrieval according to the manufacturer's protocol (Fig. 4, S5 and S8). Sections were blocked using protein block (Dako). Following blocking, sections were incubated at 4°C overnight with primary antibody diluted in antibody diluent (Dako). Primary antibody concentrations were as follows: anti-phospho-Histone H2AX 1:250 (9718, Cell Signaling), anti-CC3 1:300 (9661, Cell Signaling), and anti-Ki67 1:1000 (ab15580, Abcam). Sections were washed and then incubated with secondary antibody for 30 min at room temperature in the same antibody diluent (Dako). Secondary antibodies included Alexa-Fluor 488 donkey anti-rabbit 1:500 (A-21206, ThermoFisher) for tumor staining and Alexa-Fluor 594 (A-11012, ThermoFisher) for SI staining. Sections for IF staining were washed with PBS, counter-stained with DAPI (1 μg/mL) in PBS, washed, and coverslip-mounted using fluorescent mounting media (Dako). Fluorescent images were acquired using a Nikon Eclipse Ni-E microscope, with Nikon Plan Fluor 40x/1.30 objective for tumor tissues and 20x/0.75 objective for SI, Andos Zyla sCMOS camera, and NISElements Advanced Research software.

Multiplexed staining of SI tissue for CC3 and γ-H2AX (Fig. 3) was performed using the Opal protocol as described previously[12]. Slides were deparaffinized in xylene and rehydrated in ethanol. Slides were placed in a 1:10 dilution of ARF buffer in deionized water (Perkin Elmer) and antigen retrieval was performed in an Antigen EZ-Retreiver v. 3.0 microwave oven. Sections were blocked using protein block (Dako) and then incubated at 4°C overnight in a 1:1000 dilution of anti-phospho-histone H2A.X (γ-H2AX) antibody (9718, Cell Signaling). Protein detection was performed using the ImmPRESS® HRP Anti-Rabbit IgG (Peroxidase) Polymer Detection Kit (Vector Laboratories) followed by incubation in a 1:100 dilution of Opal 570 (FP1488001KT, Perkin Elmer). Antigen retrieval and blocking steps were repeated and slides were incubated at 4°C overnight in a 1:1000 dilution of anti-CC3 antibody (9661, Cell Signaling). The secondary antibody was the same as used for (γ-H2AX) followed by incubation in a 1:100 dilution of Opal 520 (FP1487001KT, Perkin Elmer). Tissues were washed with PBS, counter-stained with DAPI (1 μg/mL) in PBS, washed, and coverslip-mounted using fluorescent mounting media (Dako). Fluorescent images were acquired using a Nikon Eclipse Ni-E microscope, with Nikon Plan Fluor 20x/0.75 objective, Andos Zyla sCMOS camera, and NISElements Advanced Research software. Only those epithelial cells directly aligning the crypt were quantitated.

Statistical Analysis.

The statistical analyses used in this study are described in each figure legend. Log-Rank analysis was used for survival studies and median survival was determined with 95% confidence interval (CI). Two tailed t-tests with unequal variance were used to compare the number of regenerating crypts per circumference of SI and for quantitating the immunofluorescence staining of SI. Tukey's multiple comparison test with a single pooled variance of a one-way ANOVA was used to compare crypt depth, crypts per mm, villi height, traced crypts, and for quantiting the immunofluorescence staining of tumor tissue. Values less than 0.05 were considered significant.

Results

Fasting protects wild-type mice from radiation-induced death

To determine if fasting-mediated chemoprotection[5] can be generalized to radiation treatment, 9-week-old C57BL/6J mice were either fed *ad libitum* or fasted for 24 h and then exposed to TA-XRT at 11.5 Gy, which was identified as the maximum tolerated dose in fasted-irradiated mice (Fig. S1). TA-XRT was performed using a circular 25 mm field to the abdomen placed below the xiphoid process (Fig. S2) to ensure radiation of the entire intestinal tract while sparing nearly all the bone marrow in the pelvis, thereby avoiding competing hematopoietic toxicity. After radiation, mice were returned to their cages with free access to food and water and were monitored for 30 days, during which time food intake and body weight were recorded (Fig. 1A). All fed mice died between days 6 and 7. In contrast, all of the animals that were fasted prior to radiation exposure survived for 30 days, the study endpoint (Fig. 1B). Fed animals decreased their food intake until time of death which occurred at day 6–7 and was due to radiation-induced toxicity. Food intake began to increase by day 7 in fasted mice, peaking at day 11 and eventually stabilizing at 4 g/day up to day 30 (Fig. 1C). Body weight decreased steadily in fed mice from original body weight until death at day 6–7. In contrast, fasted animals lost approximately 20% of their body weight during the 24 h fast period, but refeeding resulted in a 10% regain of original body weight by day 3 followed by a steady decline until day 7. By day 14, these mice had regained most of their original weight and maintained or increased it until study endpoint (Fig. 1D). Both groups showed general signs of radiation toxicity, including decreased activity, ruffled fur, and hunched back posture but at day 8, the fasted group started to revert to healthy activity levels.

Fasting protects SI stem cells, enabling recovery of SI epithelium after radiation

To examine the effects of pre-radiation fasting on intestinal stem cell regeneration after radiation we performed traditional microcolony assays (Fig. 2A and B), which demonstrated a significantly greater number of regenerating crypts per circumference in the fasted group relative to the fed group (Fig. 2C). To further evaluate the effects of the TA-XRT field on the mice, abdominal organs were harvested from fed and fasted mice at day 6 post-radiation. SI tissues from irradiated mice showed significant damage compared to those of unirradiated mice (Fig. 2D). Specifically, SI from irradiated mice showed hypertrophic crypts and shortened villi compared to unirradiated controls. Moreover, the number of crypts per mm of intestine was significantly greater in the SI of the fasted-irradiated group than in those of the

fed-irradiated group (Fig. 2E). The greater number of crypts per mm of intestine suggested that fasting protected SI stem cells.

Results from microcolony assays as well as the presence of hypertrophic crypts, suggested that fasting protected SI stem cells from high-dose radiation. Stem cell reporter mice were used to test which stem cell populations were responsible for epithelial repopulation following radiation damage. Knock-in mice carrying tamoxifen-inducible Cre under the transcriptional control of the mouse *Lgr5* promoter to mark crypt base columnar (CBC) stem cells[13] or the *Bmi1* promoter to mark the supra-Paneth (+4) stem cell pool[14] were bred to mice carrying the floxed-stop *Rosa26-LacZ* reporter (R26R) to induce permanent LacZ expression, mark $Lgr5^+$ or $Bmi1^+$ cells, and enable lineage tracing. Fed and fasted mice were treated with TA-XRT followed by tamoxifen at 1 and 3 h post-radiation. SI tissues were isolated on day 6, stained for LacZ expression (Fig. 2F), and traced crypts per area were quantified (Fig. 2G). Although traced crypts were observed in both *Lgr5* and *Bmi1* reporter mice, fasting only significantly increased those in *Lgr5* reporter mice.

Because mice in both fed and fasted groups exhibited radiation-induced toxicity at day 6 (Fig. 1), we evaluated intestinal tissues at different time points within the observed 30-day survival timeline to evaluate whether intestinal epithelium recovery correlated with mouse health. Intestinal tissues were harvested from both fed- and fasted-irradiated mice at day 4 as well as at days 10 and 30 from fasted-irradiated groups (Fig. S3). At day 4, an appreciable decrease in the number of crypts per mm was noted in the fed-radiated group as compared to the fasted-irradiated group (Fig. S3B). This decrease was maintained through day 6. Additionally, villi blunting occurred between days 4 and 6. Both these measures correlated with declining animal health in fed and fasted cohorts for up to 7 days in the fasted-irradiated group and until death in the fed-radiated group (Fig. 1). In fasted mice, intestinal epithelium regeneration was observed by day 10, as evidenced by increased crypts per mm of intestine, increased villi length, and decrease crypt hypertrophy. Intestinal recovery at day 10 correlated with improved health in fasted-irradiated mice and their subsequent survival.

Fasted-irradiated and fasted-control mice were followed for 180 days to determine if short-term fasting protected mice from the long-term side-effects associated with high-dose radiation (Fig. S4A). At D180 one mouse in the fasted-irradiated group was found deceased. The remaining mice were euthanized and their kidneys, livers, spleens, pancreata and SI were isolated. Although most fasted-irradiated mice weighed less than fasted-unirradiated mice at the time of euthanasia, the difference was not significant (Fig. S4B). Pancreatic tissue was found in only one of the three remaining fasted-irradiated mice and their SI were thicker and more rigid than those isolated from fasted non-irradiated mice. By gross examination, livers, kidneys and spleens were indistinguishable between irradiated and non-irradiated cohorts.

Next, tissue sections were stained with hematoxylin and eosin (H & E) and trichrome for microscopic evaluation. There were no significant differences in crypt depth, villi height or number of crypts per mm of SI between the fasted-irradiated and fasted-unirradiated groups indicating a recovery of the SI epithelial compartment following the original radiation insult (Fig. S4C–D). However, submucosal fibrosis was observed in the SI of fasted-irradiated

mice. Microscopic evaluation of remaining pancreatic tissue from the one irradiated mouse where pancreatic tissue could be found, revealed fibrosis and loss of exocrine pancreas. By contrast, fibrosis was not detected in the spleens, kidneys or livers of fasted-irradiated mice (Fig. S4E).

Separate cohorts of fed or fasted mice that had been radiated or not were euthanized and their SI harvested at different timepoints and stained with antibodies specific for γH2AX and CC3 to evaluate DNA damage and cell death (Fig. 3A). There were no significant differences in the number of crypt epithelial cells staining positive for γH2AX between fed and fasted cohorts at any of the evaluated timepoints (Fig. 3B). These results indicate that in SI crypts, fasting on its own did not induce DNA damage, nor did it significantly impact the generation or resolution of DNA damage following radiation. Although there were no differences in the number of crypt epithelial cells staining positive for γH2AX in fed and fasted mice 24h post-radiation (Fig. 3B), there were reduced levels of CC3 staining in the crypts of fasted mice (11.492% positive crypt cells) when compared to fed mice (16.891% positive crypt cells) (Fig. 3C). These results indicate that fasting may protect SI crypt cells from IR-induced apoptosis or that apoptotic cells were cleared more readily in fasted animals. There were no significant differences in Ki67 staining between fed or fasted cohorts at any of the evaluated timepoints (Fig. S5).

Pre-radiation fasting does not reduce tumor response to radiation

The response of malignant and normal cells to genotoxic stress is differentially affected by fasting[4,15,16]. Fasting chemosensitizes tumors[4,15,16] while protecting normal tissues against toxicity. To determine the effects of fasting on the radiation responses of pancreatic cancer, we employed a syngeneic orthotopic KPC model of pancreatic cancer, using cells with a heterozygous *Trp53* loss-of-function mutation and an activated *Kras* allele[17]. KPC cells were implanted into the pancreata of C57BL/6J mice, and tumors became established over 2 weeks as detected by ultrasound imaging (Fig. 4A and Fig. S6). After tumors were confirmed, animals were randomized to four treatment groups: fed-unirradiated, fasted-unirradiated, fed-irradiated, and fasted-irradiated. Mice were either fed or fasted for 24 h, then irradiated with a single dose of TA-XRT (12 Gy) or not, and returned to their cages with food. Ultrasound imaging was performed every 4–5 days to monitor tumor growth and animals were euthanized due to excessive tumor burden or an observed general health decline, as per IACUC guidelines (Fig. 4A).

Fasting alone did not significantly affect the median survival of unirradiated tumor-bearing mice (Fig. 4B). When combined with TA-XRT, fasting significantly increased median survival (to 43 days) when compared to fed-irradiated tumor-bearing mice (7 days, Log rank P=0.0021) and modestly increased median survival when compared to fasted-unirradiated tumor-bearing mice (13 days, Log rank P=0.0231, Fig. 4B). Tumors in the fasted-irradiated group consistently showed a lag in growth following radiation, thereby prolonging survival in this group (Fig. 4B and S7).

To further evaluate the effects of fasting on tumor cells treated with radiation, we grew orthotopic KPC tumors and subjected the mice to fed or fasted conditions after tumors had grown to an efficient size for measurements. Mice were then irradiated or not and tumors

were harvested either immediately or 24 h post-radiation. Tumor tissues were stained with antibodies specific for either γH2AX (Fig. 4C) or CC3 (Fig. S8A). Baseline levels of γH2AX were similar in fed and fasted-unirradiated tumors. Tumors harvested from fed and fasted mice immediately after radiation had similarly high levels of γH2AX. Together these results suggested that fasting alone did not induce DNA damage nor reduce the capacity of radiation to induce DNA damage in tumors. Moreover, levels of γH2AX were significantly higher in the 24 h post radiation tumors of fasted mice relative to their fed cohorts (Fig. 4D) indicating that fasting prior to radiation reduced the capacity of pancreatic tumors to repair the DNA double strand breaks induced by IR. There were no significant differences in CC3 levels between fed and fasted tumors at any time point (Fig. S8B).

SI were isolated from tumor bearing mice at the time of euthanasia to examine tissue integrity (Fig. 4E). Fed-irradiated mice that died within 10 days of irradiation (8/9 mice, 88.9%) showed severely atrophic SI epithelia (Fig, 4E). There were fewer crypts per mm of jejunum, blunted villi, and more hypertrophic crypts compared to unirradiated controls and fasted-irradiated mice (Fig 4F). In contrast, fasted-irradiated mice that survived initial radiation-induced toxicity (7/8, 87.5%), displayed abundant crypts per mm and healthy-looking villi. In comparison, SI from unirradiated controls were normal (Fig. 4E and F).

Because most of the animals in the fed-irradiated group were euthanized due to radiation-induced GI toxicity (Table S1), the effect of fasting on tumor response to radiation could not be fully examined. Therefore, we utilized an intramuscular tumor model in which KPC tumor cells were injected in the hind leg of mice (Fig. S9A). By radiating only the hind limb, we eliminated competing death from GI toxicity. Although radiation caused a minor lag in tumor growth when compared to unirradiated controls, there were no significant differences in tumor growth between the fed and fasted groups (Fig. S9B).

Discussion

In this study, we describe how a 24 h fast promoted intestinal stem cell regeneration and organismal survival after a lethal dose of abdominal radiation. This protection appears to be limited to normal tissues, as pancreatic tumors were not radioprotected and may have even demonstrated a mild, but selective increase in radiation damage, as measured by γ-H2AX foci. The mechanism of this effect may be from reduced early apoptosis in normal tissues, but not tumors.

We developed a novel TA-XRT model using a 25 mm circular collimator that targeted intestinal tissue while sparing most of the bone marrow in the thorax and pelvis. This enabled us to impart GI toxicity without invoking competing hematopoietic toxicity. We note that very little toxicity was observed in mice that survived otherwise lethal radiation, with limited intestinal and pancreatic fibrosis. We also used this large field to treat pancreatic tumors, which led to improved outcomes only when coupled with a short term fast for radioprotection. Thus, despite these excellent outcomes, we note that these experiments only demonstrate proof of principle for fasting-mediated radioprotection to enable ablative RT. Future clinical studies should use smaller fields such as those used in

stereotactic body radiotherapy (SBRT), which would further reduce both acute and chronic radiation-induced sequelae.

Two distinct stem cell populations have been thoroughly described in the SI. Lgr5+ stem cells reportedly replenish the SI epithelium during homeostatic turnover of villi cells[13] while Bmi1+ stem cells are more quiescent under normal physiological conditions[14]. After radiation, Bmi1+ stem cells proliferate and have the capacity to produce Lgr5+ stem cells and repopulate the SI epithelium[14]. It has also been shown that although Lgr5+ stem cells are radiosensitive, complete depletion prior to radiation impairs intestinal epithelial recovery. This suggests that Lgr5+ stem cells are also required for crypt epithelial cell regeneration post damage[18]. In the context of fasting-mediated SI radioprotection, we provided evidence that both Lgr5+ and Bmi1+ intestinal stem cells contributed to regeneration of the SI following high dose radiation.

Additional studies have also shown that other intestinal cell types including $Dll1^+$ secretory progenitors[19], label retaining cells[20], Alpi expressing enterocyte precursors[21], $Krt19^+$ progenitor cells[22], enteroendocrine[23], and Paneth cells[24,25] are capable of de-differentiating when the stem cell compartment is compromised. Furthermore, a recent study employing single cell RNA sequencing identified a novel multipotent SI stem cell, deemed revival stem cells, marked by high clusterin expression that undergoes transient expansion following irradiation. These revival stem cells were shown to reconstitute the Lgr5 compartment following ablation with diphtheria toxin and to facilitate intestinal regeneration after experimentally-induced colitis[26]. Future studies should interrogate the contribution made by each these cell populations to crypt epithelial cell recovery following ionizing radiation under fed and fasted conditions. Furthermore, experiments should investigate the generalizability of our SI observations to other stem cell niches like skin and bone marrow.

Several clinical trials have monitored the effects of fasting on the response of cancer patients to therapy. One study randomized women with stage II/III breast cancer into a short-term fast 24 h before and after the start of their chemotherapy regimen or a control arm of regular nutrition. In this study, short term fasting was well tolerated and reduced chemotherapy-induced hematological toxicities[27]. Another study evaluated different fasting periods, from 24–72 h, prior to platinum-based chemotherapy. Decreased DNA damage was observed in the leukocytes of patients who fasted over 48 h. This study also showed that fasting up to 72 h was feasible and induced minor side-effects including fatigue, headache, and dizziness[28].

It has been approximated that a 24 h fast in mice correlates to a one week water-only diet in humans[8]. Many patients who receive SBRT already fast for extended periods of time to reduce filling of the stomach and duodenum[29]. However, we do not envision that fasting beyond 24 hours would be advisable in pancreatic cancer patients, many of whom are already underweight and/or cachectic. Identifying the molecular mechanisms underlying the potent and selective radioprotection afforded by fasting could lead to the identification of a drug mimetic that could be employed instead of having to persistently reduce dietary intake in this already frail patient population.

Fasting-induced downregulation of IGF-1 has been proposed as one mechanism to explain how fasting provides chemoprotection to normal but not tumor tissue[4]. IGF-1 deficient mice survive longer than wild-type when exposed to lethal doses of a variety of chemotherapies including cyclophosphamide, 5-fluoroacil and doxorubicin[4]. Contrary to these observations, reduction in the circulating levels of IGF-1 was shown to sensitize, rather than protect, non-tumor bearing mice to etoposide treatment[4]. Fasting-mediated protection from lethal doses of etoposide is driven, in part, by increased SI stem cell survival, which correlates with their enhanced ability to repair DNA double strand breaks[5]. It has also been demonstrated that caloric restriction, a prolonged reduction in caloric intake, augments the repair of sublethal damage in normal tissues[30]. Caloric restriction has been shown to upregulate proteins involved in non-homologues end joining (NHEJ) like XLF and Ku[31,32]. Additionally, the deacetylase SIRT1, which binds and deacetylates Ku70 thereby enhancing DSB repair, has been shown to have increased activity during caloric restriction. While in our data evaluating whole crypts, we did not observe significant changes in DNA damage resolution, we cannot discard the possibility that differences between fed and fasted animals would be detected if we assayed specific stem cell populations (for example Lgr5+ or Bmi1+ stem cells) since these cells compose a minority of the cells in the crypt.

Future studies should aim to identify molecular mechanisms of fasting-induced GI protection from chemotherapy and radiation therapy. A detailed understanding of the biological changes that occur in stem cells during fasting and after genotoxic stress could help identify candidate drugs to mimic fasting-induced protection.

Supplementary Material

Refer to Web version on PubMed Central for supplementary material.

Acknowledgements:

We thank members of the Piwnica-Worms' and Taniguchi Labs for critical input throughout the course of this study. Anirban Maitra is thanked for providing the KPC cell line. Support to HPW came from the National Cancer Institute of the National Institutes of Health under award number R01CA207236. Support to MCB came from T32CA186892, F31CA210631 and U54CA096300/297. CMT was supported by funding from the Cancer Prevention & Research Institute of Texas (CPRIT) grant RR140012, V Foundation (V2015–22), Sidney Kimmel Foundation, Sabin Family Foundation Fellowship, and the McNair Family Foundation. This work was also supported by the NIH/NCI under award number P30CA016672 for use of the Small Animal Imaging Facility. HPW is an American Cancer Society Research Professor.

Conflict of Interest Statement: MCB, KMS, SJJ, TNF, JM, GMAT, XZ, CMT, and HPW report grants from National Cancer Institute during the conduct of this study. TNF and CMT report grants from the Cancer Prevention and Research Institute of Texas during the conduct of this study. The authors have declared that no conflict of interest exists. CMT reports additional grants from V Foundation, Sidney Kimmel Foundation, Sabin Family Foundation and McNair Family Foundation during the conduct of this study. RBB has nothing to disclose.

References

1. Siegel R, Ma J, Zou Z, et al. Cancer statistics, 2014. CA Cancer J Clin 2014;64:9–29. [PubMed: 24399786]
2. Von Hoff DD, Ramanathan RK, Borad MJ, et al. Gemcitabine plus nab-paclitaxel is an active regimen in patients with advanced pancreatic cancer: A phase i/ii trial. J Clin Oncol 2011;29:4548–54. [PubMed: 21969517]

3. Ben-Josef E, Schipper M, Francis IR, et al. A phase i/ii trial of intensity modulated radiation (imrt) dose escalation with concurrent fixed-dose rate gemcitabine (fdr-g) in patients with unresectable pancreatic cancer. International journal of radiation oncology, biology, physics 2012;84:1166–71.
4. Lee C, Safdie FM, Raffaghello L, et al. Reduced levels of igf-i mediate differential protection of normal and cancer cells in response to fasting and improve chemotherapeutic index. Cancer Res 2010;70:1564–72. [PubMed: 20145127]
5. Tinkum KL, Stemler KM, White LS, et al. Fasting protects mice from lethal DNA damage by promoting small intestinal epithelial stem cell survival. Proc Natl Acad Sci U S A 2015;112:E7148–54. [PubMed: 26644583]
6. Safdie FM, Dorff T, Quinn D, et al. Fasting and cancer treatment in humans: A case series report. Aging (Albany NY) 2009;1:988–1007. [PubMed: 20157582]
7. Safdie F, Brandhorst S, Wei M, et al. Fasting enhances the response of glioma to chemo- and radiotherapy. PLoS One 2012;7:e44603. [PubMed: 22984531]
8. Klement RJ, Champ CE. Calories, carbohydrates, and cancer therapy with radiation: Exploiting the five r's through dietary manipulation. Cancer metastasis reviews 2014;33:217–29. [PubMed: 24436017]
9. Fujimoto TN, Colbert LE, Huang Y, et al. Selective egln inhibition enables ablative radiotherapy and improves survival in unresectable pancreatic cancer. Cancer Res 2019;79:2327–2338. [PubMed: 31043430]
10. Molkentine JM, Fujimoto TN, Horvath TD, et al. Enteral activation of wr-2721 mediates radioprotection and improved survival from lethal fractionated radiation. Scientific reports 2019;9:1949. [PubMed: 30760738]
11. Withers HR, Elkind MM. Microcolony survival assay for cells of mouse intestinal mucosa exposed to radiation. Int J Radiat Biol Relat Stud Phys Chem Med 1970;17:261–7. [PubMed: 4912514]
12. Stack EC, Wang C, Roman KA, et al. Multiplexed immunohistochemistry, imaging, and quantitation: A review, with an assessment of tyramide signal amplification, multispectral imaging and multiplex analysis. Methods 2014;70:46–58. [PubMed: 25242720]
13. Barker N, van Es JH, Kuipers J, et al. Identification of stem cells in small intestine and colon by marker gene lgr5. Nature 2007;449:1003–7. [PubMed: 17934449]
14. Yan KS, Chia LA, Li X, et al. The intestinal stem cell markers bmi1 and lgr5 identify two functionally distinct populations. Proc Natl Acad Sci U S A 2012;109:466–71. [PubMed: 22190486]
15. Raffaghello L, Lee C, Safdie FM, et al. Starvation-dependent differential stress resistance protects normal but not cancer cells against high-dose chemotherapy. Proc Natl Acad Sci U S A 2008;105:8215–20. [PubMed: 18378900]
16. Lee C, Raffaghello L, Brandhorst S, et al. Fasting cycles retard growth of tumors and sensitize a range of cancer cell types to chemotherapy. Science translational medicine 2012;4:124ra27.
17. Hingorani SR, Wang L, Multani AS, et al. Trp53r172h and krasg12d cooperate to promote chromosomal instability and widely metastatic pancreatic ductal adenocarcinoma in mice. Cancer Cell 2005;7:469–83. [PubMed: 15894267]
18. Metcalfe C, Kljavin NM, Ybarra R, et al. Lgr5+ stem cells are indispensable for radiation-induced intestinal regeneration. Cell Stem Cell 2014;14:149–59. [PubMed: 24332836]
19. van Es JH, Sato T, van de Wetering M, et al. Dll1+ secretory progenitor cells revert to stem cells upon crypt damage. Nat Cell Biol 2012;14:1099–1104. [PubMed: 23000963]
20. Buczacki SJ, Zecchini HI, Nicholson AM, et al. Intestinal label-retaining cells are secretory precursors expressing lgr5. Nature 2013;495:65–9. [PubMed: 23446353]
21. Tetteh PW, Basak O, Farin HF, et al. Replacement of lost lgr5-positive stem cells through plasticity of their enterocyte-lineage daughters. Cell Stem Cell 2016;18:203–13. [PubMed: 26831517]
22. Asfaha S, Hayakawa Y, Muley A, et al. Krt19(+)/lgr5(−) cells are radioresistant cancer-initiating stem cells in the colon and intestine. Cell Stem Cell 2015;16:627–38. [PubMed: 26046762]
23. Yan KS, Gevaert O, Zheng GXY, et al. Intestinal enteroendocrine lineage cells possess homeostatic and injury-inducible stem cell activity. Cell Stem Cell 2017;21:78–90 e6. [PubMed: 28686870]
24. Yu S, Tong K, Zhao Y, et al. Paneth cell multipotency induced by notch activation following injury. Cell Stem Cell 2018;23:46–59 e5. [PubMed: 29887318]

25. Schmitt M, Schewe M, Sacchetti A, et al. Paneth cells respond to inflammation and contribute to tissue regeneration by acquiring stem-like features through scf/c-kit signaling. Cell reports 2018;24:2312–2328 e7. [PubMed: 30157426]
26. Ayyaz A, Kumar S, Sangiorgi B, et al. Single-cell transcriptomes of the regenerating intestine reveal a revival stem cell. Nature 2019.
27. de Groot S, Vreeswijk MP, Welters MJ, et al. The effects of short-term fasting on tolerance to (neo) adjuvant chemotherapy in her2-negative breast cancer patients: A randomized pilot study. BMC Cancer 2015;15:652. [PubMed: 26438237]
28. Dorff TB, Groshen S, Garcia A, et al. Safety and feasibility of fasting in combination with platinum-based chemotherapy. BMC Cancer 2016;16:360. [PubMed: 27282289]
29. Colbert LE, Rebueno N, Moningi S, et al. Dose escalation for locally advanced pancreatic cancer: How high can we go? Adv Radiat Oncol 2018;3:693–700. [PubMed: 30370371]
30. Heydari AR, Unnikrishnan A, Lucente LV, et al. Caloric restriction and genomic stability. Nucleic Acids Res 2007;35:7485–96. [PubMed: 17942423]
31. Um JH, Kim SJ, Kim DW, et al. Tissue-specific changes of DNA repair protein ku and mthsp70 in aging rats and their retardation by caloric restriction. Mech Ageing Dev 2003;124:967–75. [PubMed: 14499502]
32. Lee JE, Heo JI, Park SH, et al. Calorie restriction (cr) reduces age-dependent decline of non-homologous end joining (nhej) activity in rat tissues. Experimental gerontology 2011;46:891–6. [PubMed: 21821112]

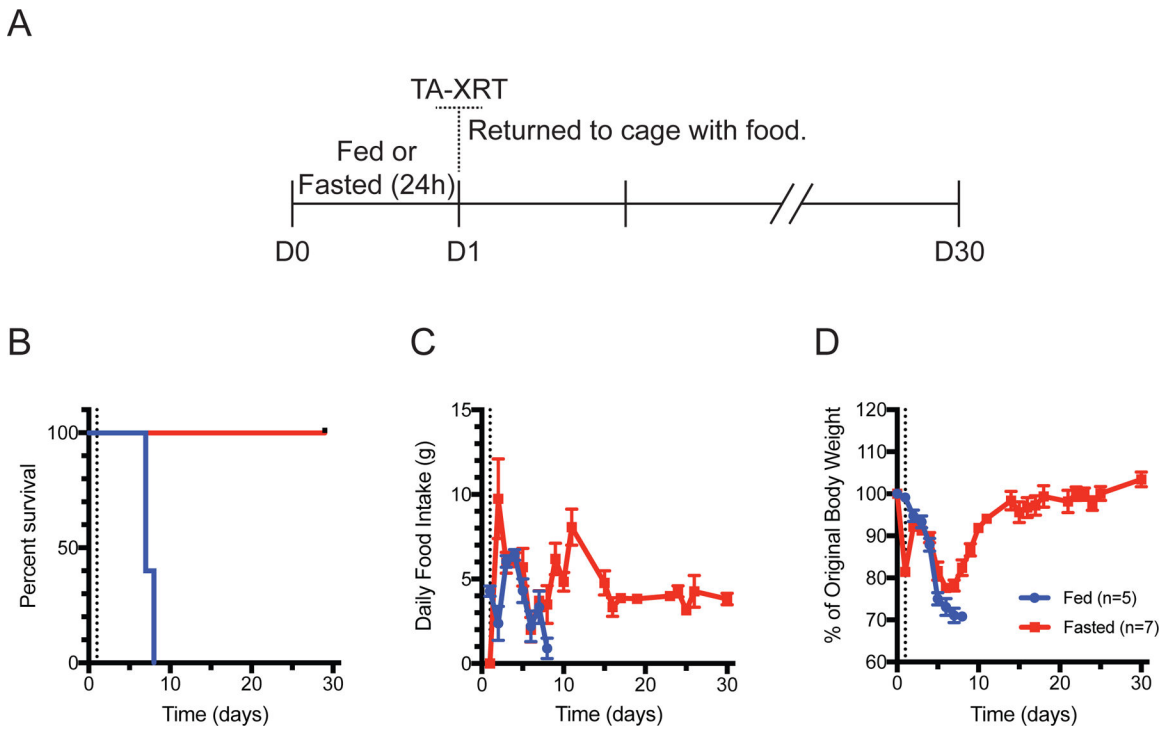

Figure 1:

Twenty-four hour fasting protects mice from radiation-induced death. (A) C57Bl/6J mice were allowed to feed *ad libitum* or were fasted for 24 h. Total abdominal radiation (TA-XRT; 11.5 Gy) was administered (day 1). Mice were returned to single-housed cages with food. (B) Survival was monitored daily. (C) Daily food intake and (D) individual mouse body weights were measured. All error bars are ± SEM.

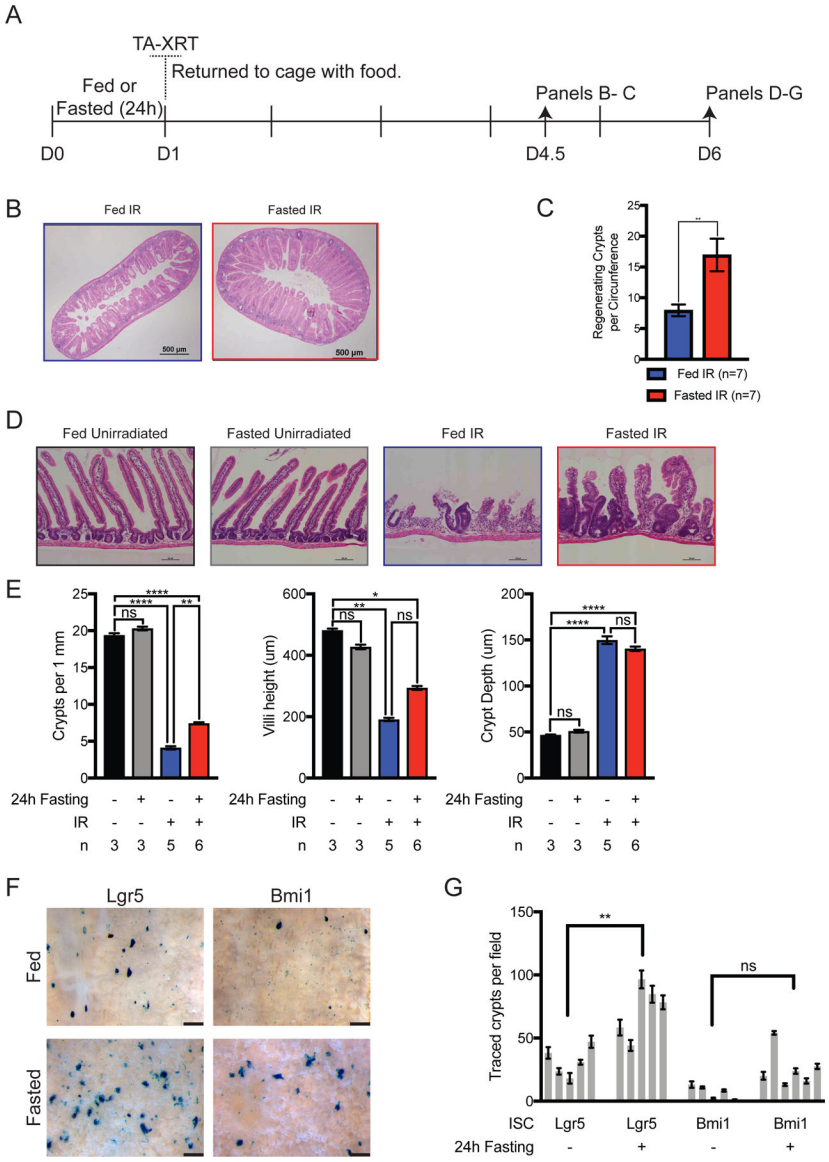

Figure 2:

Fasting protects SI stem cells from high dose radiation. (A) C57Bl/6J mice were treated as shown. (B) Representative images of hematoxylin and eosin (H & E)-stained SI (day 4.5). Scale bars, 500 μm. Magnification, 4x. (C) Regenerating crypts per circumference were quantified in 4 separate sections of intestine and the average per mouse was plotted. The Student *t*-test was performed for comparison of groups (n = 7 per group, p=0.0077). Error bars are ± SEM. (D) Representative images of H & E-stained SI (day 6). Scale bars, 100 μm. Magnification, 10x. (E) Quantification of H & E data. Crypt depth and villi height (n=50 per mouse) were measured and plotted. Number of crypts per length (n=30 fields per mouse) of SI was quantified for each sample and number of crypts per millimeter of SI length plotted. *P<0.05; **P<0.005, ****P<0.0001 by Tukey post-test of a one-way ANOVA. Error bars are ± SEM. (F) Reporter mice were administered two doses of tamoxifen (t) 1 and 3 h after radiation. Mice were euthanized on D6, SI were harvested and whole-mount tissue stained

for LacZ expression. Villi were removed from a 3-cm section of LacZ-stained whole-mount tissue for counting traced crypts. Representative images are shown. (Scale bars, 500 μm) (G) The number of fully traced crypts per field of view in whole-mount images was quantified, individual mice plotted. **P<0.005 by Holm-Sidak's multiple comparison of a one-way ANOVA. Error bars are ± SEM.

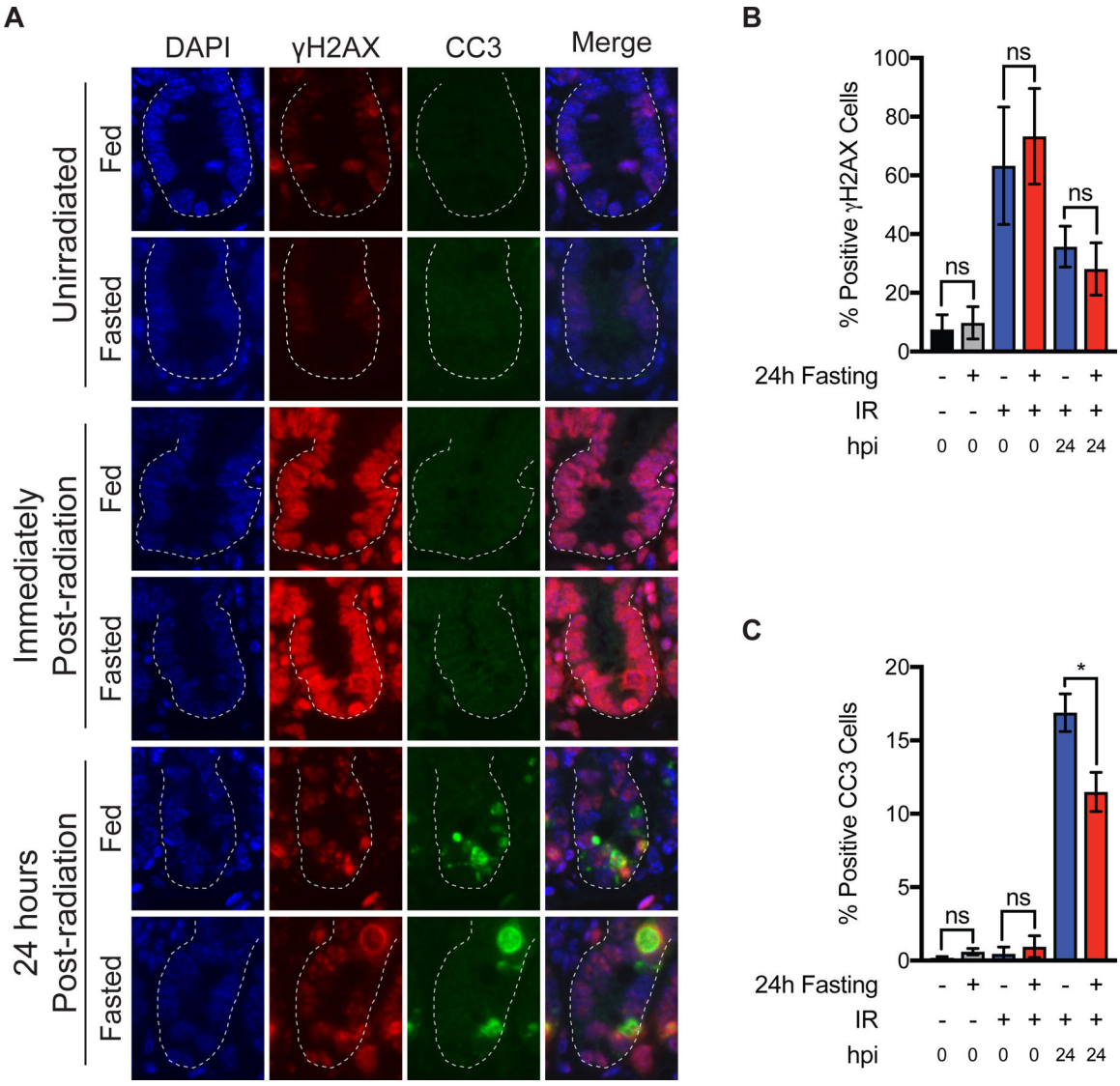

Figure 3:

Effects of pre-radiation fasting on IR-induced DNA damage and apoptosis. (A) C57Bl/6J mice were allowed to feed *ad libitum* or were fasted for 24 h. Unirradiated SI tissues were harvested at this time. Other cohorts were radiated with TA-XRT (11.5Gy) and SI tissues harvested either immediately or 24 h after radiation (hpi= hours post irradiation). SI tissues (jejunum) were analyzed for γH2AX and cleaved caspase-3 (CC3) by immunofluorescence staining. Representative images are shown. Scale bars, 10 μm. Magnification, 20x. (B) Positive γH2AX cells per crypt were quantified (30 crypts per mouse, n=4 mice per treatment group and mean per treatment plotted. ns= not significant by student's t-test. Error bars are ± SEM. (C) Positive cleaved caspase-3 cells per crypt were quantified (30 crypts per mouse, n=4 mice per treatment group and mean per treatment plotted. ns= not significant; *P<0.05 by student's t-test. Error bars are ± SEM.

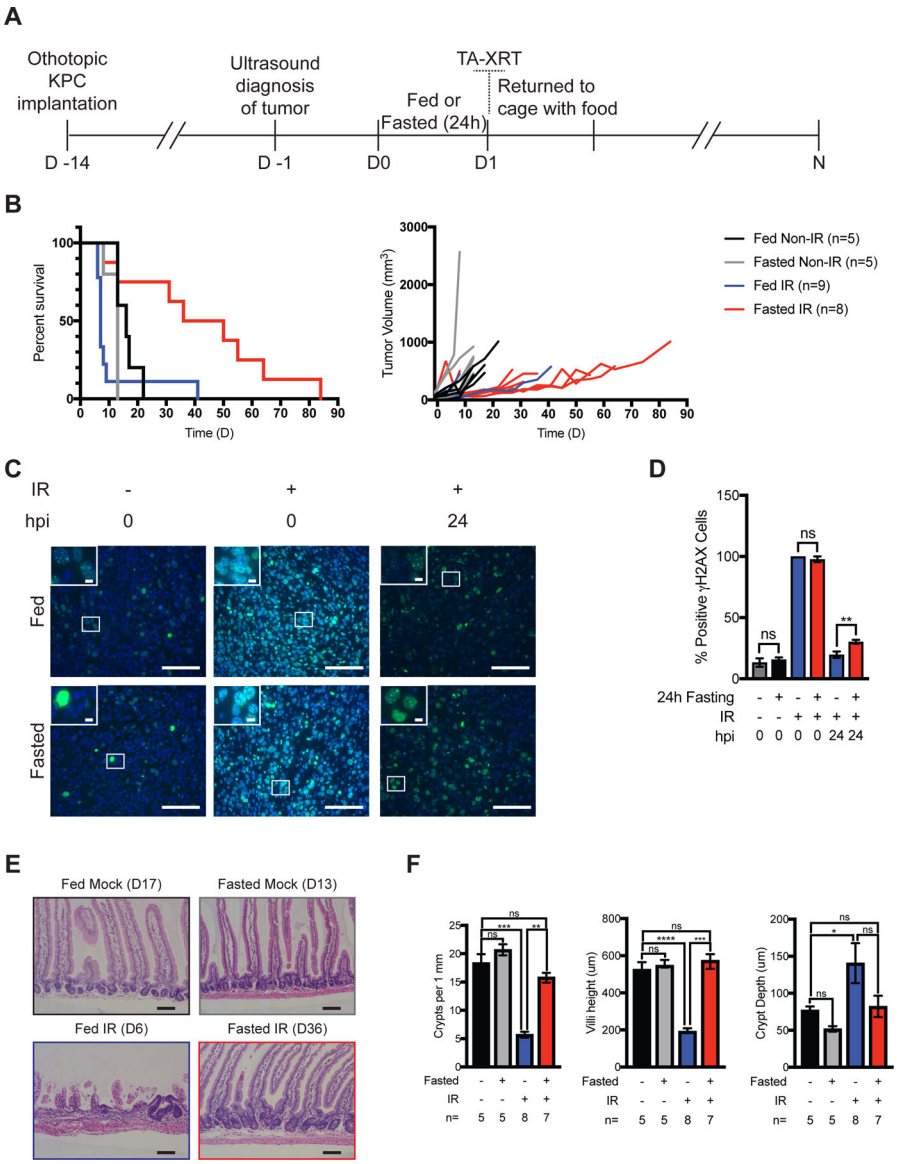

Figure 4:

Pre-radiation fasting does not confer protection to orthotopic KPC pancreatic tumors. (A) KPC cells (2×10^5) were orthotopically injected into 12-week-old C57Bl/6J mice. Two weeks later, tumors were measured using ultrasound and mice were randomized into four treatment groups. Mice were allowed to feed or were fasted for 24 h. Total abdominal radiation (TA-XRT; 12 Gy) was administered (day 1). Access to food was restored immediately after treatment. Ultrasound tumor measurements were taken every 4–5 days until death. (B) Survival was monitored daily. Tumor growth curves for individual mice are shown. Bonferroni corrected Log-rank test. (C) Pancreatic tumor-bearing mice were treated as indicated (hpi = hours post irradiation) and tumors were analyzed for γH2AX by immunofluorescence staining. Representative images are shown. (D) Positive cells per field were quantified (5 fields per mouse, n=3 mice per treatment) and average per treatment was plotted. Scale bars, 100 μm. Magnification, 40x. Inset scale bars, 20 μm. **P<0.005 by

Tukey post-test of a two-way ANOVA. Error bars are ± SEM. (E-F) Representative images of H & E-stained jejunum from tumor-bearing mice harvested at the time of euthania (as indicated). Scale bars, 100 μm. Magnification, 10x. Crypt depth and villi heights (n = 50 per mouse) were measured and average value per treatment group plotted. Number of crypts per length of SI as quantified for each sample (n=30 fields per mouse) and average number of crypts per millimeter of SI length plotted. *P<0.05; **P<0.005, ***P<0.005, ****P<0.0001 by Tukey post-test of a one-way ANOVA. Error bars are ± SEM.